JACS
JOURNAL OF THE AMERICAN CHEMICAL SOCIETY
pubs.acs.org/JACS
Article

Optical Control of G-Actin with a Photoswitchable Latrunculin

Nynke A. Vepřek, Madeline H. Cooper, Laura Laprell, Emily Jie-Ning Yang, Sander Folkerts, Ruiyang Bao, Malgorzata Boczkowska, Nicholas J. Palmer, Roberto Dominguez, Thomas G. Oertner, Liza A. Pon, J. Bradley Zuchero, and Dirk H. Trauner*

Cite This: J. Am. Chem. Soc. 2024, 146, 8895−8903
Read Online

ACCESS | Metrics & More | Article Recommendations | Supporting Information

ABSTRACT: Actin is one of the most abundant proteins in eukaryotic cells and is a key component of the cytoskeleton. A range of small molecules has emerged that interfere with actin dynamics by either binding to polymeric F-actin or monomeric G-actin to stabilize or destabilize filaments or prevent their formation and growth, respectively. Among these, the latrunculins, which bind to G-actin and affect polymerization, are widely used as tools to investigate actin-dependent cellular processes. Here, we report a photoswitchable version of latrunculin, termed opto-latrunculin (**OptoLat**), which binds to G-actin in a light-dependent fashion and affords optical control over actin polymerization. **OptoLat** can be activated with 390−490 nm pulsed light and rapidly relaxes to its inactive form in the dark. Light activated **OptoLat** induced depolymerization of F-actin networks in oligodendrocytes and budding yeast, as shown by fluorescence microscopy. Subcellular control of actin dynamics in human cancer cell lines was demonstrated via live cell imaging. Light-activated **OptoLat** also reduced microglia surveillance in organotypic mouse brain slices while ramification was not affected. Incubation in the dark did not alter the structural and functional integrity of the microglia. Together, our data demonstrate that **OptoLat** is a useful tool for the elucidation of G-actin dependent dynamic processes in cells and tissues.

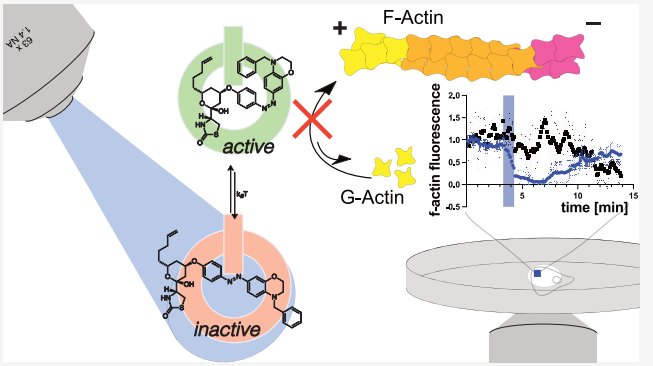

INTRODUCTION

Actin is one of the most abundant proteins in eukaryotic cells and is essential to their integrity and dynamics. The actin cytoskeleton is maintained through a dynamic interplay between globular, monomeric G-actin and filamentous, polymeric F-actin (Figure 1a). This homeostasis is regulated by numerous actin binding proteins that are involved in a wide variety of signaling cascades.[1−3] Actin dynamics can also be altered by small molecules, which can have stabilizing or destabilizing effects on F-actin.[4] Stabilizers, such as phalloidin and jasplakinolide, bind to the filaments and prevent depolymerization.[5−7] In essence, they function as molecular glues that tie together three actin protomers. The cytochalasins bind to the terminal monomers on a filament (barbed end), preventing further polymerization.[8] Among the actin destabilizing natural products, latrunculins A and B stand out by their unique binding site and mechanism of action. Latrunculins A and B bind G-actin in the nucleotide binding cleft between subdomains 2 and 4 (Figure 1b,c).[9] The binding of latrunculin in this site prevents conformational changes that are crucial for the incorporation of G-actin into the polymerizing filament.[9] In a sense, they function as "intramolecular glues" between subdomains 2 and 4 that change the interactome of G-actin and prevent its polymerization.[10] The main mechanism of action is, therefore, the sequestration of actin monomers. Additionally, latrunculin A can be involved in the active severing of filaments.[11]

The study of actin dynamics in cells and tissues is challenging, because of the many factors that control the remodeling of the dynamic actin networks. To address some of these challenges, we have previously introduced photoswitchable versions of the actin stabilizer jasplakinolide that allow for the reversible stabilization of actin filaments with subcellular precision.[12,13]

Although jasplakinolide-based probes have been used to study the effect of F-actin stabilization on cytoskeletal function, actin dynamics in cells also depend on the highly regulated G-actin pool.[14] G-actin dependent remodeling of actin, for instance, during cell migration, takes place within seconds-minutes.[15] The investigation of such processes requires tools that allow for modulation of the G-actin pool at the time scales of the biological processes under investigation. Here, we

Received: October 3, 2023
Revised: February 28, 2024
Accepted: February 29, 2024
Published: March 21, 2024

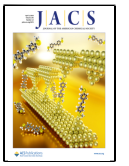

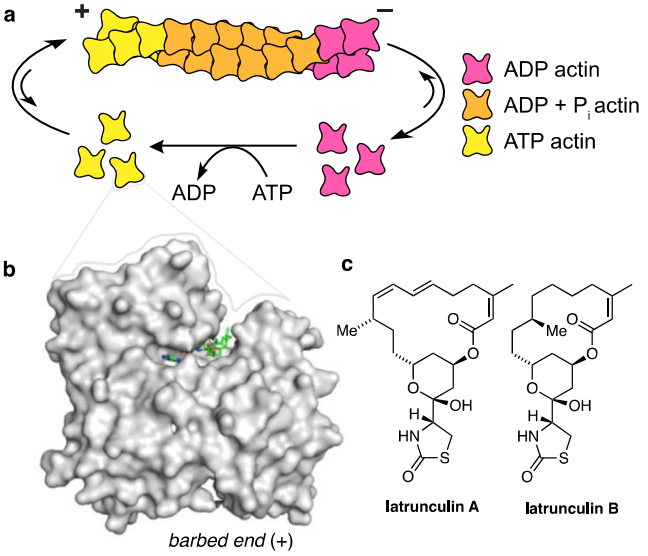

Figure 1. Actin turnover is inhibited by binding of latrunculin to G-actin. a) Schematic representation of actin turnover (treadmilling). b) Latrunculins bind ATP-G-actin above the nucleotide binding cleft (PDB: 2q0u). c) Chemical structures of latrunculins A and B.

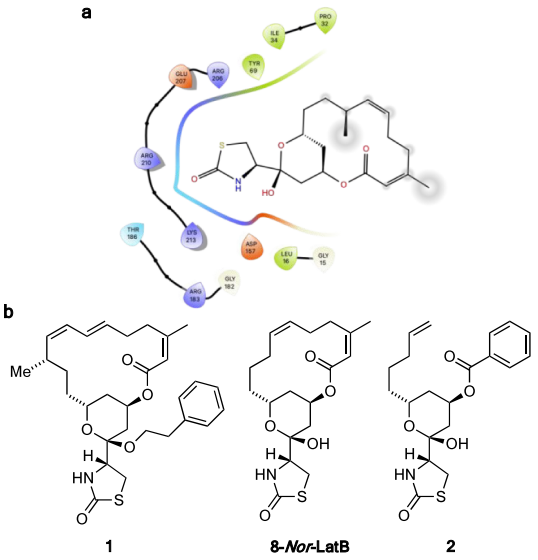

Figure 2. a) Interactions of latrunculin B with the G-actin. b) Chemical structures of modified or truncated latrunculins identified in SAR studies.

describe optical probes that are complementary to the F-actin stabilizers previously introduced and derived from the G-actin binders, latrunculins A and B. Our photoswitchable version of latrunculin, **OptoLat**, can sequester G-actin monomers in a light dependent, reversible fashion leading to spatially and temporally confined breakdown of actin networks. We show that actin dynamics can be altered not only in cultured human cancer cell lines with **OptoLat**, but also in mammalian oligodendrocytes and microglia, as well as the budding yeast *Saccharomyces cerevisiae*.

RESULTS

Design and Synthesis. We based the design of optolatrunculins on published X-ray crystal structures and known structure−activity relationship studies.[16−20] Latrunculins bind G-actin right next to the nucleotide binding cleft between subdomains 2 and 4 and inhibit the conformational twist that is essential for incorporation of ATP-bound G-actin into F-actin (Figure 2a).[9] Their thioazolidinone core and hemiacetal engage in hydrogen bonding with the protein whereas the lipophilic macrocycle is predominantly involved in hydrophobic interactions (Figure 2a).[19−21]

Structure−activity relationship studies have identified certain modifications of latrunculins that retain bioactivity. For instance, acetal **1**, derived from latrunculin itself was shown to inhibit actin polymerization at 1.0 μM concentration in biochemical studies.[18] The fully synthetic derivative, **8-*Nor*-latrunculin B,** was found to cause actin disruption at μM concentrations.[22] *Seco* derivatives such as the benzoate **2** were also found to be active, albeit with slightly reduced potency.[22]

Based on this knowledge, we designed the photoswitchable derivatives shown in Figure 3a. These include photoswitchable acetals such as **3** and **4**, which retain the macrocycle and were based on **1**, as well as azobenzene and diazocine esters such as **5** and **6**, inspired by **2**. To increase the steric clash between the molecule and protein by photoisomerization of the diazine bond, we also installed *meta* and *ortho* derivatives **7** and **8**. Concerned about the stability of esters, we explored derivatives bearing aryl ethers that had not been previously described. In addition to metabolic stability, aryl ethers would also bring the photoswitch deeper into the protein pocket, which could increase steric effects. To this end, we synthesized azobenzenes **9** and **10** and diazocine **11**. In the next iteration, we aimed at increasing the bulk of the photoswitch by introducing different functionalities such as oxirane, trimethoxy, and *N*-benzyl aryls on the photoswitch, generating aryl ethers **12**−**15**. Among these **14**, bearing a *para N*-benzyl azobenzene photoswitch, emerged as the most useful compound and was termed **OptoLat**.

The synthesis of **OptoLat** (**14**) (Figure 3b) started with a titanium tetrachloride mediated aldol addition of enantiomerically pure aldehyde **16** to PMB-protected thioazolidinone **17**. As described by Fürstner, acid-mediated silyl deprotection resulted in cyclization and gave a separable (1.25:1) mixture of hemiacetals (*S*) and (*R*)-**19**.[23] (*S*)-**19** was converted into the methyl acetal following oxidative PMB deprotection.[16,23] Subsequent Mitsunobu reaction with azobenzene **21** under optimized conditions using TMAD, followed by hydrolysis, gave **OptoLat** in a good overall yield (48% over 2 steps).

Photoswitchable acetals **3** and **4** were procured from the corresponding hemiacetals as described in the Supporting Information. Aryl ethers **5**−**6** were made by Mitsunobu reactions from (*S*)-**19**. Ether derivatives **9**, **11**−**13**, and **15** were obtained by similar synthetic strategies as **OptoLat**. **10** was accessed by S_NAr from (*R*)-**19**.

Initial Photophysical and Biological Evaluation. All photoswitchable latrunculins were characterized for their photophysical properties to determine appropriate illumination conditions (Supporting Information). Due to its *para* amino substituent, **OptoLat** showed the most red-shifted absorption spectrum (λ_{max} *trans* ca. 450 nm) and fastest thermal relaxation ($t_{1/2}$ < 2 s in DMSO).[24,25] *trans* **OptoLat** can be efficiently activated with wavelengths between 390 and 490 nm (Figure 4e). The activation efficiency was determined by NMR with *in situ* irradiation using ultra high-power LEDs (see Supporting Information). The highest ratio of the *cis* isomer was reached at 460 nm (ca. 67%). Upon irradiation with 390 nm ca. 49% *cis*

https://doi.org/10.1021/jacs.3c10776
J. Am. Chem. Soc. 2024, 146, 8895−8903

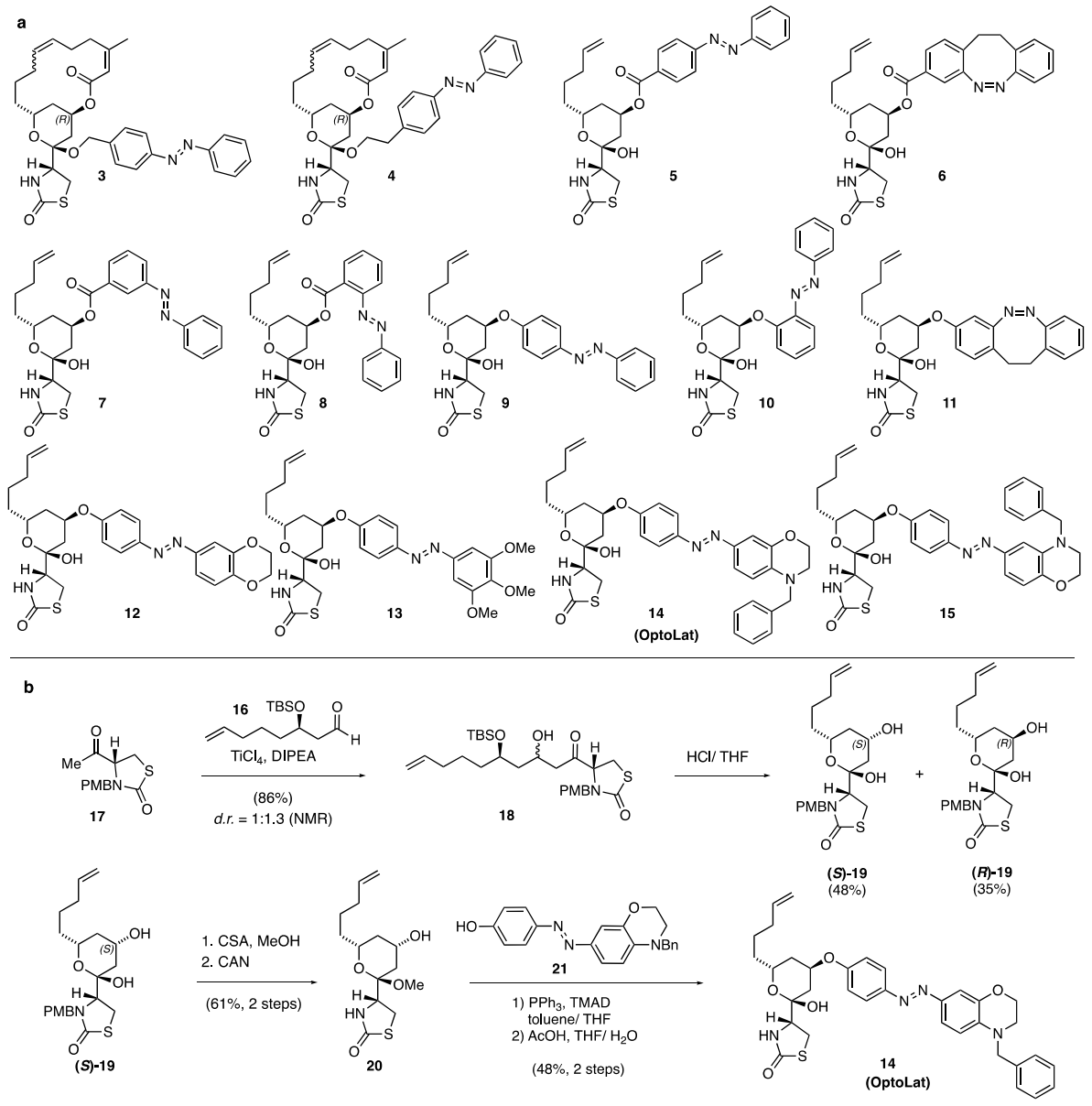

Figure 3. Photoswitchable latrunculin derivatives and the synthesis of OptoLat. a) Photoswitchable latrunculin derivatives synthesized. b) Synthetic route toward OptoLat (14).

and 520 nm ca. 26% *cis* were obtained (Figure 4f). The *cis* isomer was short-lived ($t_{1/2}$ ca. 1.6 s, Figure 4g) which resulted in complete deactivation of the photoswitch in the absence of light within seconds. Switching was fully reversible and did not show fatigue (Figure S9).

Next, we evaluated our photoswitches using light-dependent cell proliferation (MTT) assays in HeLa cells. Acetals **3** and **4**, derived from phenethyl latrunculin A (**1**), were found to be completely inactive. *Seco* esters **5**−**8**, proved to be active, albeit with high EC_{50} values compared to macrocyclic reference compounds (e.g., **8**-*Nor*-**latB**). However, they did not produce any light-dependent antiproliferative activity. Their methyl acetals, which are synthetic intermediates, were completely inactive (**5 OMe** and **7 OMe**). Azoaryl ether **9** showed a small difference in light versus dark activity (Figure 3b). However, other modifications of the photoswitch including the incorporation of an *ortho* azobenzene (**10**) and a diazocine (**11**), as well as more bulky substituents in **12** and **13** did not lead to a widening in the photopharmacological window. This was also true for "*iso*-Optolat" **15** which has increased steric bulk by virtue of its benzyl substituent. Gratifyingly, its isomer **OptoLat** (**14**), which has desirable photophysical and thermal properties, proved to be less active in the dark, even at high concentrations, but became highly active upon irradiation with blue light (Figure 4c). Therefore, our detailed biological investigations focused on this photoswitchable form of latrunculins A and B. Cell proliferation assays across different cell lines showed that **OptoLat** has an EC_{50} of about 3 μM (see SI). As such, it is about three times less active than **latrunculin B** itself. Compared to **8**-*Nor*-**lat B**, however, **OptoLat** showed 2.5 times higher antiproliferative activity in our HeLa assays (Figure 4a,c).

To assess the ability of **OptoLat** to inhibit actin polymerization, we performed pyrene-actin polymerization assays with N-WASP WCA-activated Arp2/3 complex in the presence of activated or nonactivated **OptoLat** (under 465 nm light or in

https://doi.org/10.1021/jacs.3c10776
J. Am. Chem. Soc. 2024, 146, 8895−8903

a

compound	λ (*trans-cis*)	EC_{50} (light)	EC_{50} (dark)	Δ
3	370 nm	>100 μM	>100 μM	–
4	370 nm	>100 μM	>100 μM	–
5 OMe	370 nm	>100 μM	>100 μM	–
5	370 nm	39.2 μM	39.4 μM	–
6	400 nm	20.4 μM	28.7 μM	–
7 OMe	370 nm	>100 μM	>100 μM	–
7	370 nm	35.6 μM	38.2 μM	–
8	370 nm	33.4 μM	37.0 μM	–
9	390 nm	20.4 μM	32.9 μM	+
10	380 nm	25.4 μM	>25 μM	–
11	410 nm	19.4 μM	27.8 μM	–
12	390 nm	36 μM	40 μM	–
13	390 nm	31.2 μM	32.1 μM	–
14	440 nm	3.1 μM	>100 μM	++
15	380 nm	19 μM	28.8 μM	–
latrunculin A	N/A	N/A	0.1 μM	
latrunculin B	N/A	N/A	1.6 μM	
8-*Nor*-Lat B	N/A	N/A	14 μM	

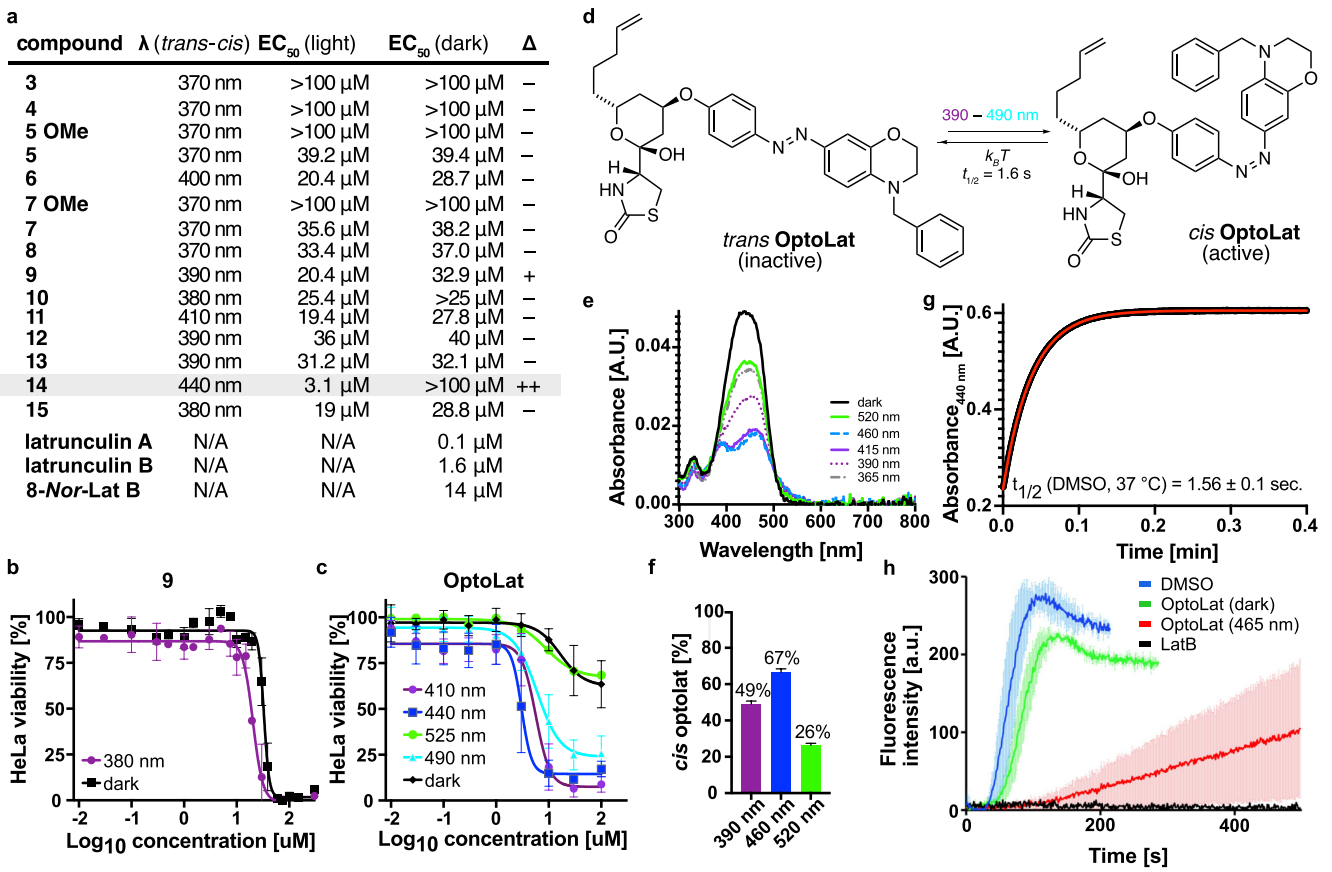

Figure 4. Initial biological evaluation with cell proliferation assays and the photophysical properties of **OptoLat**. a) Antiproliferative activity of photoswitchable latrunculin analogs and reference compounds. b) Cell viability dose−response curves for 9 under dark and illuminated conditions. c) Cell viability dose−response curves for **OptoLat** (14) under illumination with different wavelengths and in the dark. d) Photochemical and thermal isomerization of **OptoLat**. e) UV−vis absorption spectrum of **OptoLat**. f) Percentage of *cis* **OptoLat** measured by NMR with *in situ* irradiation at different wavelengths. g) Thermal relaxation of *cis* OptoLat in the dark in DMSO solution at 37 °C. h) Time-course of actin polymerization under the following conditions: 2 μM actin (6% pyrene-labeled), 100 nM bovine Arp2/3 complex, 400 nM N-WASP WCA with the addition of 20 μM nonactivated (dark) **OptoLat** (green), 20 μM activated (465 nm light) **OptoLat** (red), or 20 μM LatB (black), or DMSO (blue) as controls. Data are shown as the average curve from three independent experiments with SD error bars in lighter color.

the dark, respectively). Compared to controls with added DMSO (full polymerization) and LatB (inhibited polymerization), **OptoLat** produced a light-dependent inhibition of polymerization, which decayed slowly over time (Supporting Information and Figure 4h).

Shaping Actin-Based Structures in Oligodendrocytes and Budding Yeast Cells. Next, we investigated whether the strong antiproliferative effect indeed resulted from the destabilization of actin networks in different cell types. HeLa cells treated with **OptoLat** and kept in the dark showed normal actin structures, which broke down upon pulsed irradiation with 410 nm within 24 h. The quantification of these results, however, was difficult since breakdown of the actin network also affects the size and shape of HeLa cells. We therefore turned to oligodendrocytes, glial cells that develop extensive actin networks during their maturation but do not require actin to maintain their structural integrity.[26] This feature makes them an ideal cell type for testing actin perturbing agents like **OptoLat**. We treated rat oligodendrocytes with escalating doses of **OptoLat**. Following 6 h of **OptoLat** activation (pulsed irradiation with 430 nm), we observed a significant decrease in filamentous actin at all **OptoLat** doses as measured by phalloidin staining (Figure 5a). The degree of actin disassembly was similar to the degree of disassembly seen in response to treatment with 100 nM latrunculin A (Figure 5b). We observed no difference between levels of filamentous actin in oligodendrocytes treated with **OptoLat** that were kept in the dark, or DMSO, demonstrating the lack of basal activity of *trans* **OptoLat**.

Since actin is highly conserved across species, we wondered whether **OptoLat** is also active in yeast cells. In budding yeast (*Saccharomyces cerevisiae*), there are three major actin-containing structures: actin patches, contractile rings, and actin cables. Actin patches are endosomes bearing an F-actin coat that localize to the bud (daughter cell).[27] Contractile rings drive separation of mother and daughter cells during cell division, in yeast as in other eukaryotes, and localize to the bud neck. Actin cables are actin bundles that assemble in the bud and extend along the mother-bud axis. They are essential for cell proliferation for their function as tracks for transport of organelles and other cellular constituents from mother to daughter cells during cell division.[28,29] Finally, actin cables are dynamic structures that undergo rapid turnover and treadmilling from their site of assembly in the bud toward the mother cell.[30] As a result, they are highly sensitive to the destabilization by latrunculin.[31]

One of the advantages of a fast-relaxing photoswitchable actin destabilizer is that it could allow for the modulation of

https://doi.org/10.1021/jacs.3c10776
J. Am. Chem. Soc. 2024, 146, 8895−8903

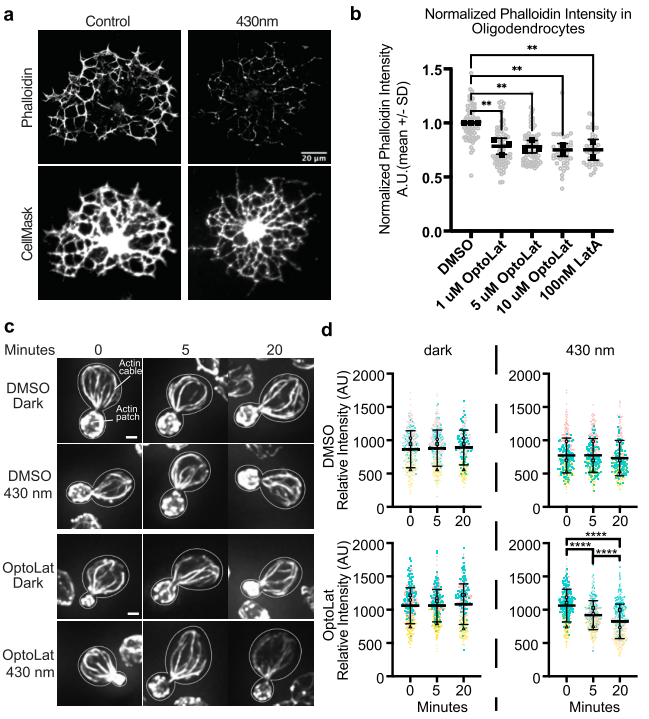

Figure 5. Light-dependent reduction of actin content using **OptoLat**. a) Depletion of F-actin in oligodendrocytes visualized using phalloidin staining after irradiating with 430 nm light. b) Quantification of F-actin depletion in oligodendrocytes. ** $p \leq 0.01$, values were calculated using one-way ANOVA followed by Dunnett's multiple comparison test. c) Mid-log-phase yeast cells were incubated in the presence or absence of 100 μM **OptoLat** in the dark or upon exposure to pulsed blue light (430 nm) for 0−20 min. Cells were then fixed and stained for F-actin using AlexaFluor488 (AF488)-phalloidin. Maximum projections of the actin cytoskeleton in the presence and absence of **OptoLat** activation. Cell outlines are shown in white. Scale bar: 1 μm. d) Quantitation of AF488-phalloidin-stained F-actin in actin cables. Results are given as the mean ± standard deviation (SD) from 3 independent trials. $n > 80$ cells/time point/condition/trial. The mean (large symbols) and all data points (small symbols) of 3 independent trials are shown, with differently shaped and colored symbols for each trial. Statistical significance was determined by the two-way ANOVA, with Tukey's multiple comparisons test. **** $p \leq 0.0001$.

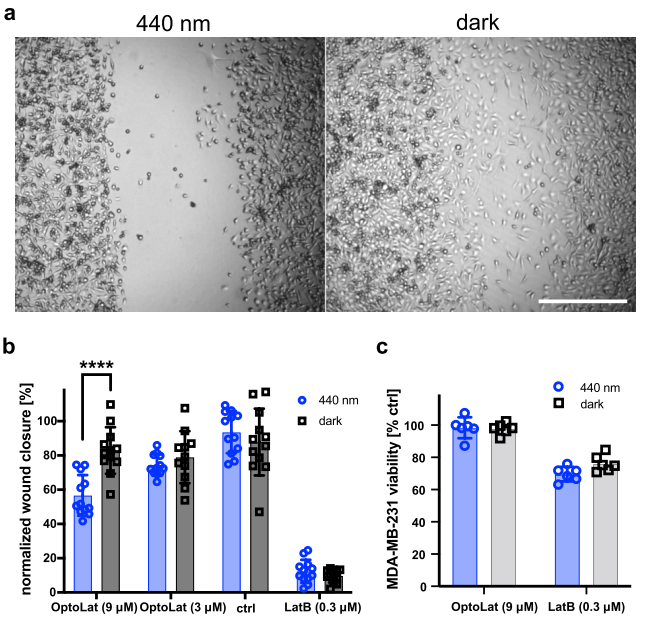

Figure 6. Light-dependent wound closure of MDA-MB-231 cells. a) Representative images of wound closure under irradiation with 440 nm and in the dark. Scale bar = 500 μm. b) Quantification of wound closure after 24 h (**OptoLat** 9 μM, 3 μM, control and latrunculin B at 0.3 μM). c) Cell viability after 48 h under treatment conditions (**OptoLat** 9 μM, latrunculin B 0.3 μM). Irradiation protocol 25 ms pulses every 1 s. ****$p \leq 0.0001$. Statistical analysis was performed using Mann−Whitney test.

actin dynamics with temporal precision. Therefore, we monitored the effect of **OptoLat** on yeast actin cables by measuring the fluorescence intensity of F-actin in fluorochrome-coupled phalloidin-stained actin cables. Treatment of budding yeast cells with **OptoLat** in the dark, with DMSO in the dark, or with illumination at 430 nm had no detectable effect on actin cables. By contrast, activation of **OptoLat** with pulsed blue light (430 nm) resulted in a rapid, time-dependent decrease in the F-actin content in actin cables (Figure 5c,d). Indeed, we observed a significant decrease in actin cables within 5 min of **OptoLat** activation and a further decrease in those structures after 20 min of **OptoLat** activation.

Wound Healing Assays. Since the remodeling of actin networks is essential to cell migration,[32−35] we next investigated whether **OptoLat** reduces the migration of invasive cancer cells in a light-dependent fashion, without showing significant toxicity. In a wound healing assay, **OptoLat** did not affect wound closure in the dark (Figure 6). Under pulsed-irradiated conditions, however, **OptoLat** significantly reduced wound closure. *cis* **OptoLat** was not cytotoxic at concentrations that strongly impaired cell migration (9 μM, 24 h, 440 nm) (Figure 6c).

Reversible Perturbation of Actin Dynamics in Networks in Live Cells. The actin networks in lamellipodia show very high turnover rates as these are required to drive cell migration.[32−34] To further assess the temporal and spatial precision of **OptoLat**, we investigated the ability of **OptoLat** to modulate the actin dynamics in the lamellipodia of migrating cells with subcellular resolution. MDA-MB-231 cells that stably express mCherry LifeAct, a fluorescent protein that labels F-actin,[36] were incubated with **OptoLat** overnight and kept in the dark. Under these conditions, the cells were directly compared to vehicle controls and behaved normally. The local pulsed irradiation of a region of interest (ROI) in the lamellipodium led to a reduction of protrusion dynamics, which was followed by a breakdown of the actin network. Upon keeping the cells in the dark, actin networks fully recovered (Figure 7, Supplementary Movie). This recovery was quantified through normalization of the LifeAct fluorescence in the ROI (Figure 7b). F-actin fluorescence was steeply reduced upon **OptoLat** activation. The destructed network persisted for several minutes before a full recovery was observed. Irradiation with 440 nm light alone did not lead to the destruction of the actin network in control cells (Figure 7, DMSO control). The dynamic changes of actin turnover upon light irradiation can also be clearly visualized by using kymographs (Figure 7c).

Effects on Microglia in Brain Slices. Having shown that **OptoLat** was effective in cultured cells, we tested whether our novel tool could also be applied in complex tissues. As an example, we investigated microglial surveillance activity in organotypic brain slices in the presence of **OptoLat** under dark- and light-activated conditions. Microglia are highly branched immune cells that constantly scan the brain

https://doi.org/10.1021/jacs.3c10776
J. Am. Chem. Soc. 2024, 146, 8895−8903

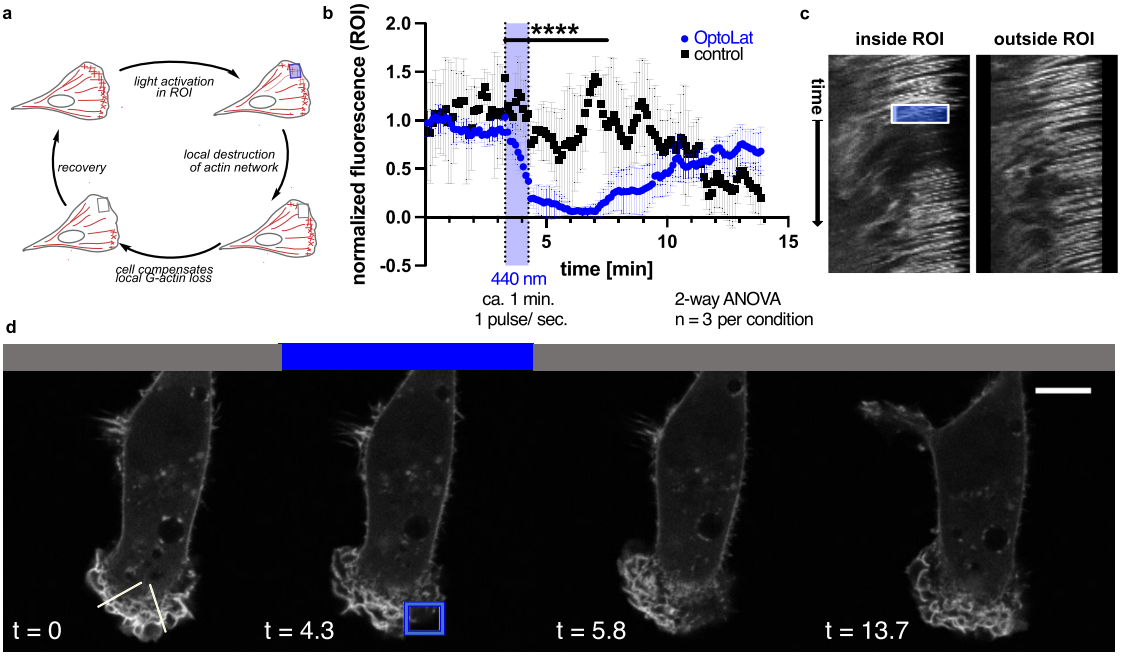

Figure 7. Cell migration and local subcellular remodeling of actin networks. a) Schematic of local **OptoLat** activation, actin network destruction, and recovery. ROI = region of irradiation. b) Quantification of fluorescence inside and outside the ROI for n = 3 per condition. Black squares = region outside of the ROI; blue circles = within the ROI. c) Kymographs inside and outside of the ROI along the yellow lines in d). The box represents the duration and extent of irradiation in the ROI. d) Time course images of a representative cell treated with **OptoLat**. Yellow lines in the left panel indicate selections for the kymographs (left: outside of the ROI; right: within the ROI). Scale bar = 10 μm; **OptoLat** concentration used: 30 μM.

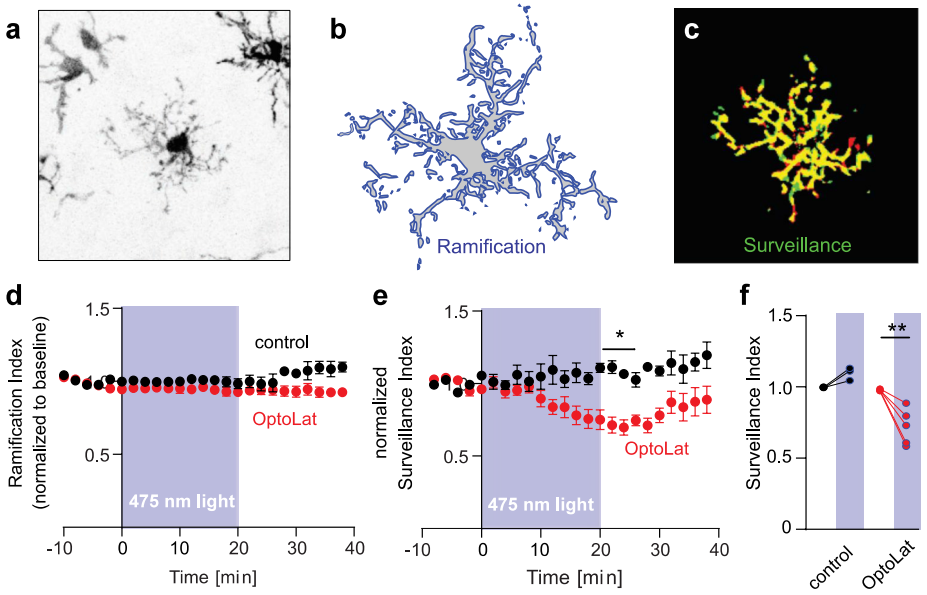

Figure 8. Light-induced reduction of microglia surveillance in a brain slice culture. a) Fluorescence image (contrast inverted) of microglia in hippocampal tissue culture expressing tdTomato. b) Ramification of microglia was calculated by dividing its perimeter by the surface area. c) Surveillance was quantified as the sum of areas covered only at one time point (red + green pixels). d) Ramification of microglia was not affected upon activation of **OptoLat**. Red: tissue incubated with **OptoLat** and illuminated for 20 min. Black: tissue without **OptoLat**, illuminated for 20 min. Mean ± SEM, normalized to baseline. e)Surveillance index of microglia incubated with **OptoLat** (red) and without **OptoLat** (black). Reduction of surveillance after ca. 10 min irradiation in the presence of **OptoLat**, followed by recovery. Mean ± SEM, normalized to baseline. f) Statistical analysis of light-induced changes in surveillance index in cultures without (control, n = 3 cells/slice cultures) and with **OptoLat** (n = 5 cells/slice cultures). Baseline (−10 to 0 min) was compared to postlight period (20−22 min). 2-way ANOVA with Bonferroni post hoc test. Adjusted p-value: 0.0028. **OptoLat** concentration used: 30 μM.

parenchyma by extending and retracting filopodia-like structures (surveillance). These processes are highly dynamic and depend on actin remodeling, while the overall shape of the cell (ramification) depends on microtubule networks.[37]

https://doi.org/10.1021/jacs.3c10776
J. Am. Chem. Soc. 2024, 146, 8895−8903

To investigate whether **OptoLat** affects the behavior of microglial cells, we prepared hippocampal slice cultures from mice expressing a red fluorescent protein exclusively in microglia (Cx3Cr1Cre-tdT). We incubated slice cultures with **OptoLat** overnight and imaged microglia 60−80 μm below the surface of the slice culture with two-photon microscopy (Figure 8a). From maximum intensity projections taken at two time points (Δt = 2 min), we quantified the cell's shape (ramification) and its motility (surveillance). The ramification index is a measure of the ratio of the cell's perimeter to its area (Figure 8b). The surveillance index is a measure of the area (pixels) surveyed per unit of time (Figure 8c). In the dark, ramification and surveillance of microglia conditioned with **OptoLat** were not different from vehicle controls. **OptoLat** activation by pulsed blue light did not affect ramification (Figure 8d), but induced a significant reduction in microglia surveillance (Figure 8e,f). The effect persisted for approximately 10 min after the light was turned off, after which surveillance slowly recovered. In the absence of **OptoLat**, pulsed blue light had no effect on surveillance (Figure 8e,f)[38] These experiments demonstrate that **OptoLat** can not only be used in single layer cell culture, but also in complex tissue. The compound is well tolerated and does not seem to trigger an adverse immune response in the dark, which would have caused the retraction of microglia processes during the **OptoLat** incubation period.

DISCUSSION

Photoswitchable modulators of the cytoskeleton allow for the light-induced precise spatial and temporal modulation of cytoskeletal dynamics. Recently, we have developed light-responsive stabilizers of F-actin derived from the natural product jasplakoinlide.[12,13] Here, we report the generation of a light-activated actin destabilizer, the photoswitchable latrunculin derivative **OptoLat**.

Our design of photoswitchable latrunculins was based on the known SAR and several X-ray structures of latrunculin A/B bound to G-actin. This also enabled computational docking studies that pointed to the need for a large photoswitch for optimal difference in activity (see Supporting Information). Congruent with our docking studies, **OptoLat** (**14**) showed a big difference in activity upon irradiation, whereas its constitutional isomer **15** did not. The systematic evaluation of candidates with the desired photophysical and thermal properties ultimately resulted in the most effective compound, **OptoLat**. This blue-light sensitive, fast-relaxing photoswitch allows for the disassembly of actin structures with high spatiotemporal precision. It is cell permeant and performs well in a variety of cell types, such as yeast cells, human cancer cell lines, rodent oligodendrocytes, and microglia embedded in rodent brain slices. It extends the toolset available for the temporally and spatially restricted modulation of actin dynamics and complements other optogenetic[39,40] and photopharmacological[12,13] approaches toward controlling the actin cytoskeleton. Its ease of application, enabled by its inactivity in the dark and its rapid, reversible activation by irradiation with blue light, opens a myriad of possible applications, from *in vitro* and cellular assays to the investigation of actin dynamics in more complex tissues or organisms.

Finally, **OptoLat** serves as a template for "latruncologs", i.e., structurally simplified latrunculin A/B derivatives that are synthetically accessible in ca. 10 steps. The stable aryl ether moiety can be introduced via Mitsunobu reaction of nucleophilic aromatic substitution, enabling the synthesis of a wide range of analogs that can be easily diversified. The systematic exploration of these analogs, which can be further functionalized, e.g., with fluorophores, is under active investigation in our laboratories.

ASSOCIATED CONTENT

Supporting Information

The Supporting Information is available free of charge at https://pubs.acs.org/doi/10.1021/jacs.3c10776.

Supplementary tables and figures, materials and methods for biological evaluation, and detailed synthesis procedures (PDF)

Supporting Movie demonstrating subcellar effects of **OptoLat** on MDA-MB-231 cells (AVI)

AUTHOR INFORMATION

Corresponding Author

Dirk H. Trauner − *Department of Chemistry, New York University, New York, New York 10003, United States; Department of Chemistry, University of Pennsylvania, Philadelphia, Pennsylvania 19104, United States;* orcid.org/0000-0002-6782-6056; Email: dtrauner@upenn.edu

Authors

Nynke A. Vepřek − *Department of Chemistry, New York University, New York, New York 10003, United States; Department of Chemistry, Ludwig Maximilian University, Munich D-80539, Germany*

Madeline H. Cooper − *Department of Neurosurgery, Stanford University School of Medicine, Stanford, California 94305, United States*

Laura Laprell − *Institute for Synaptic Physiology, ZMNH, University Medical Center Hamburg-Eppendorf, Hamburg D-20251, Germany*

Emily Jie-Ning Yang − *Department of Pathology and Cell Biology, Columbia University Irving Medical Center, New York, New York 10032, United States*

Sander Folkerts − *Department of Chemistry, New York University, New York, New York 10003, United States*

Ruiyang Bao − *Department of Chemistry, New York University, New York, New York 10003, United States;* orcid.org/0000-0002-7889-656X

Malgorzata Boczkowska − *Department of Physiology, Perelman School of Medicine, University of Pennsylvania, Philadelphia, Pennsylvania 19104, United States*

Nicholas J. Palmer − *Department of Physiology, Perelman School of Medicine, University of Pennsylvania, Philadelphia, Pennsylvania 19104, United States*

Roberto Dominguez − *Department of Physiology, Perelman School of Medicine, University of Pennsylvania, Philadelphia, Pennsylvania 19104, United States*

Thomas G. Oertner − *Institute for Synaptic Physiology, ZMNH, University Medical Center Hamburg-Eppendorf, Hamburg D-20251, Germany;* orcid.org/0000-0002-2312-7528

Liza A. Pon − *Department of Pathology and Cell Biology, Columbia University Irving Medical Center, New York, New York 10032, United States*

J. Bradley Zuchero − *Department of Neurosurgery, Stanford University School of Medicine, Stanford, California 94305, United States*

Complete contact information is available at: https://pubs.acs.org/10.1021/jacs.3c10776

Notes

The authors declare no competing financial interest.

■ ACKNOWLEDGMENTS

We thank the National Institutes of Health (Grants R01 GM126228 to D.H.T., R35 GM122589 and R33 AG051047 to L.A.P., R01 NS119823 to J.B.Z., and R01 GM073791 to R.D.) for financial support. We thank the Studienstiftung des deutschen Volkes for a PhD fellowship (to N.A.V.). We thank Prof. Anna Akhmanova (Utrecht University) for sharing the MDA-MB-231 *m*Cherry LifeAct cell line and the NYU Langone Health Microscopy Laboratory for assistance with microscopes. These studies further used the Confocal and Specialized Microscopy Shared Resource of the Herbert Irving Comprehensive Cancer Center at Columbia University Irving Medical Center, funded in part through the NIH/NCI Cancer Center Support Grant P30CA013696. We also thank the Stanford Medical Scientist Training Program (T32 GM007365-45) and Stanford Bio-X Interdisciplinary Graduate Fellowship (M.H.C.), the McKnight Endowment Fund for Neuroscience (D.H.T, J.B.Z.), the National Multiple Sclerosis Society Harry Weaver Neuroscience Scholar Award (J.B.Z.), the Myra Reinhard Family Foundation (J.B.Z.), and the Koret Family Foundation (J.B.Z.).

■ REFERENCES

(1) Dominguez, R.; Holmes, K. C. Actin Structure and Function. *Annu. Rev. Biophys.* **2011**, *40* (1), 169−186.
(2) Lee, S. H.; Dominguez, R. Regulation of Actin Cytoskeleton Dynamics in Cells. *Mol. Cells* **2010**, *29* (4), 311−326.
(3) Pollard, T. D. Actin and Actin-Binding Proteins. *Cold Spring Harb. Perspect. Biol.* **2016**, *8* (8), a018226.
(4) Allingham, J. S.; Klenchin, V. A.; Rayment, I. Actin-Targeting Natural Products: Structures, Properties and Mechanisms of Action. *Cell. Mol. Life Sci.* **2006**, *63* (18), 2119−2134.
(5) Cooper, J. A. Effects of Cytochalasin and Phalloidin on Actin. *J. Cell Biol.* **1987**, *105* (4), 1473−1478.
(6) Pospich, S.; Merino, F.; Raunser, S. Structural Effects and Functional Implications of Phalloidin and Jasplakinolide Binding to Actin Filaments. *Structure* **2020**, *28* (4), 437−449.e5.
(7) Bubb, M. R.; Senderowicz, A. M.; Sausville, E. A.; Duncan, K. L.; Korn, E. D. Jasplakinolide, a Cytotoxic Natural Product, Induces Actin Polymerization and Competitively Inhibits the Binding of Phalloidin to F-Actin. *J. Biol. Chem.* **1994**, *269* (21), 14869−14871.
(8) Scherlach, K.; Boettger, D.; Remme, N.; Hertweck, C. The chemistry and biology of chytochalasans. *Nat. Prod. Rep.* **2010**, *27*, 869−886.
(9) Morton, W. M.; Ayscough, K. R.; McLaughlin, P. J. Latrunculin Alters the Actin-Monomer Subunit Interface to Prevent Polymerization. *Nat. Cell Biol.* **2000**, *2* (6), 376−378.
(10) Schreiber, S. L. The Rise of Molecular Glues. *Cell* **2021**, *184*, 3−9.
(11) Fujiwara, I.; Zweifel, M. E.; Courtemanche, N.; Pollard, T. D. Latrunculin A Accelerates Actin Filament Depolymerization in Addition to Sequestering Actin Monomers. *Curr. Biol.* **2018**, *28* (19), 3183−3192.e2.
(12) Borowiak, M.; Küllmer, F.; Gegenfurtner, F.; Peil, S.; Nasufovic, V.; Zahler, S.; Thorn-Seshold, O.; Trauner, D.; Arndt, H.-D. Optical Manipulation of F-Actin with Photoswitchable Small Molecules. *J. Am. Chem. Soc.* **2020**, *142* (20), 9240−9249.
(13) Küllmer, F.; Vepřek, N. A.; Borowiak, M.; Nasufović, V.; Barutzki, S.; Thorn-Seshold, O.; Arndt, H.-D.; Trauner, D. Next Generation Opto-Jasplakinolides Enable Local Remodeling of Actin Networks. *Angew. Chem., Int. Ed.* **2022**, *61*, No. e2022102.
(14) Skruber, K.; Read, T.-A.; Vitriol, E. A. Reconsidering an Active Role for G-Actin in Cytoskeletal Regulation. *J. Cell Sci.* **2018**, *131* (1), jcs203760.
(15) Theriot, J. A.; Mitchison, T. J. Actin Microfilament Dynamics in Locomoting Cells. *Nature* **1991**, *352* (6331), 126−131.
(16) Fürstner, A.; Kirk, D.; Fenster, M. D. B.; Aïssa, C.; De Souza, D.; Müller, O. Diverted Total Synthesis: Preparation of a Focused Library of Latrunculin Analogues and Evaluation of Their Actin-Binding Properties. *Proc. Natl. Acad. Sci. U.S.A.* **2005**, *102* (23), 8103−8108.
(17) Fürstner, A.; Kirk, D.; Fenster, M. D. B.; Aïssa, C.; De Souza, D.; Nevado, C.; Tuttle, T.; Thiel, W.; Müller, O. Latrunculin Analogues with Improved Biological Profiles by "Diverted Total Synthesis": Preparation, Evaluation, and Computational Analysis. *Chem. -Eur. J.* **2007**, *13* (1), 135−149.
(18) Khanfar, M. A.; Youssef, D. T. A.; El Sayed, K. A. Semisynthetic Latrunculin Derivatives as Inhibitors of Metastatic Breast Cancer: Biological Evaluations, Preliminary Structure−Activity Relationship and Molecular Modeling Studies. *ChemMedchem* **2010**, *5* (2), 274−285.
(19) Allingham, J. S.; Miles, C. O.; Rayment, I. A Structural Basis for Regulation of Actin Polymerization by Pectenotoxins. *J. Mol. Biol.* **2007**, *371* (4), 959−970.
(20) Didry, D.; Cantrelle, F.-X.; Husson, C.; Roblin, P.; Moorthy, A. M. E.; Perez, J.; Le Clainche, C.; Hertzog, M.; Guittet, E.; Carlier, M.-F.; et al.et al. How a Single Residue in Individual β-Thymosin/WH2 Domains Controls Their Functions in Actin Assembly. *EMBO J.* **2012**, *31* (4), 1000−1013.
(21) Helal, M. A.; Khalifa, S.; Ahmed, S. Differential Binding of Latrunculins to G-Actin: A Molecular Dynamics Study. *J. Chem. Inf. Model.* **2013**, *53* (9), 2369−2375.
(22) Lampe, J. W.; Plourde, R., Jr.; She, J.; Vittitow, J. L.; Watson, P. S.; Crimmins, M. T.; Slade, D. J.*Cytoskeletal Active Compounds Composition and Use* US0217427A1, 2006.
(23) Fürstner, A.; Souza, D. D.; Turet, L.; Fenster, M. D. B.; Parra-Rapado, L.; Wirtz, C.; Mynott, R.; Lehmann, C. W. Total Syntheses of the Actin-Binding Macrolides Latrunculin A, B, C, M, S and 16-Epi-Latrunculin B. *Chem. −Eur. J.* **2007**, *13* (1), 115−134.
(24) Sadovski, O.; Beharry, A. A.; Zhang, F.; Woolley, G. A. Spectral Tuning of Azobenzene Photoswitches for Biological Applications. *Angew. Chem., Int. Ed.* **2009**, *48* (8), 1484−1486.
(25) Mourot, A.; Kienzler, M. A.; Banghart, M. R.; Fehrentz, T.; Huber, F. M. E.; Stein, M.; Kramer, R. H.; Trauner, D. Tuning Photochromic Ion Channel Blockers. *ACS Chem. Neurosci.* **2011**, *2* (9), 536−543.
(26) Zuchero, J. B.; Fu, M.; Sloan, S. A.; Ibrahim, A.; Olson, A.; Zaremba, A.; Dugas, J. C.; Wienbar, S.; Caprariello, A. V.; Kantor, C.; et al.etal. CNS Myelin Wrapping Is Driven by Actin Disassembly. *Dev. Cell* **2015**, *34* (2), 152−167.
(27) Huckaba, T. M.; Gay, A. C.; Pantalena, L. F.; Yang, H.-C.; Pon, L. A. Live cell imaging of the assembly, disassembly, and actin cable−dependent movement of endosomes and actin patches in the budding yeast, Saccharomyces cerevisiae. *J. Cell Biol.* **2004**, *167* (3), 519−530.
(28) Fehrenbacher, K. L.; Yang, H.-C.; Gay, A. C.; Huckaba, T. M.; Pon, L. A. Live Cell Imaging of Mitochondrial Movement along Actin Cables in Budding Yeast. *Curr. Biol.* **2004**, *14* (22), 1996−2004.
(29) Moseley, J. B.; Goode, B. L. The Yeast Actin Cytoskeleton: From Cellular Function to Biochemical Mechanism. *Microbiol. Mol. Biol. Rev.* **2006**, *70* (3), 605−645.
(30) Huckaba, T. M.; Lipkin, T.; Pon, L. A. Roles of Type II Myosin and a Tropomyosin Isoform in Retrograde Actin Flow in Budding Yeast. *J. Cell Biol.* **2006**, *175* (6), 957−969.

(31) Ayscough, K. R.; Stryker, J.; Pokala, N.; Sanders, M.; Crews, P.; Drubin, D. G. High Rates of Actin Filament Turnover in Budding Yeast and Roles for Actin in Establishment and Maintenance of Cell Polarity Revealed Using the Actin Inhibitor Latrunculin-A. *J. Cell Biol.* **1997**, *137* (2), 399−416.
(32) Pollard, T. D.; Borisy, G. G. Cellular Motility Driven by Assembly and Disassembly of Actin Filaments. *Cell* **2003**, *112* (4), 453−465.
(33) Schaks, M.; Giannone, G.; Rottner, K. Actin Dynamics in Cell Migration. *Essays Biochem.* **2019**, *63* (5), 483−495.
(34) Mitchison, T. J.; Cramer, L. P. Actin-Based Cell Motility and Cell Locomotion. *Cell* **1996**, *84* (3), 371−379.
(35) Inagaki, N.; Katsuno, H. Actin Waves: Origin of Cell Polarization and Migration? *Trends Cell Biol.* **2017**, *27* (7), 515−526.
(36) Riedl, J.; Crevenna, A. H.; Kessenbrock, K.; Yu, J. H.; Neukirchen, D.; Bista, M.; Bradke, F.; Jenne, D.; Holak, T. A.; Werb, Z.; et al.et al. Lifeact: A Versatile Marker to Visualize F-Actin. *Nat. Methods* **2008**, *5* (7), 605−607.
(37) Bernier, L.-P.; Bohlen, C. J.; York, E. M.; Choi, H. B.; Kamyabi, A.; Dissing-Olesen, L.; Hefendehl, J. K.; Collins, H. Y.; Stevens, B.; Barres, B. A.; et al.et al. Nanoscale Surveillance of the Brain by Microglia via CAMP-Regulated Filopodia. *Cell Rep.* **2019**, *27* (10), 2895−2908.e4.
(38) Laprell, L.; Schulze, C.; Brehme, M.-L.; Oertner, T. G. The Role of Microglia Membrane Potential in Chemotaxis. *J. Neuroinflammation* **2021**, *18* (1), 21.
(39) Harterink, M.; da Silva, M. E.; Will, L.; Turan, J.; Ibrahim, A.; Lang, A. E.; van Battum, E. Y.; Pasterkamp, R. J.; Kapitein, L. C.; Kudryashov, D.; et al.et al. DeActs: Genetically Encoded Tools for Perturbing the Actin Cytoskeleton in Single Cells. *Nat. Methods* **2017**, *14* (5), 479−482.
(40) Stone, O. J.; Pankow, N.; Liu, B.; Sharma, V. P.; Eddy, R. J.; Wang, H.; Putz, A. T.; Teets, F. D.; Kuhlman, B.; Condeelis, J. S.; et al.et al. Optogenetic Control of Cofilin and ATAT in Living Cells Using Z-Lock. *Nat. Chem. Biol.* **2019**, *15* (12), 1183−1190.

https://doi.org/10.1021/jacs.3c10776
J. Am. Chem. Soc. 2024, 146, 8895−8903